[Frontiers in Bioscience 16, 393-410, January 1, 2011]

Molecular imaging metrics to evaluate response to preclinical therapeutic regimens

R. Adam Smith[1], Saffet Guleryuz[1], H. Charles Manning[1-6]

[1]Vanderbilt University Institute of Imaging Science, Vanderbilt University Medical Center, Nashville, TN 37232, [2]Department of Radiology and Radiological Science, Vanderbilt University Medical Center, Nashville, TN 37232, [3]Department of Biomedical Engineering, Vanderbilt University, Nashville, TN 37232, [4]Program in Chemical and Physical Biology, Vanderbilt University Medical Center, Nashville, TN 37232, [5]Department of Neurosurgery, Vanderbilt University Medical Center, Nashville, TN 37232, [6]Vanderbilt Ingram Cancer Center, Vanderbilt University Medical Center, Nashville, TN 37232

TABLE OF CONTENTS

1. ABSTRACT

Molecular imaging comprises a range of techniques, spanning not only several imaging modalities but also many disease states and organ sites. While advances in new technology platforms have enabled a deeper understanding of the cellular and molecular basis of malignancy, reliable non-invasive imaging metrics remain an important tool for both diagnostics and patient management. Furthermore, the non-invasive nature of molecular imaging can overcome shortcomings associated with traditional biological approaches and provide valuable information relevant to patient care. Integration of information from multiple imaging techniques has the potential to provide a more comprehensive understanding of specific tumor characteristics, tumor status, and treatment response.

2. INTRODUCTION

The earlier and more accurate detection and diagnosis of cancer, as well as accompanying therapy, will doubtless be enabled by enhanced imaging procedures and diagnostic technologies. Recent progress in new technology platforms such as proteomic analysis using mass spectroscopy or gene analysis using microarrays may help identify the hallmarks of malignancy from samples of tissues or body fluids. While potentially powerful, these procedures are inherently invasive and are often plagued by sampling error and the small size of available biological samples. Thus, reliable non-invasive imaging metrics will play a major continuing role in obtaining information on the location and extent of cancer, as well as assessing tissue characteristics that can predict and interrogate treatment response and guide patient management. Hence,

considerable efforts are currently aimed at the development of improved imaging methods for the detection and evaluation of tumors, for identifying important characteristics of tumors such as the expression levels of surface receptors that may dictate what types of therapy will be effective, and for evaluating their response to treatments. Some imaging techniques depict specific cellular and molecular markers of disease, while others report on more general features such as cell density, blood flow, and metabolism which are not specific hallmarks of cancer. In this review we discuss the role of molecular and functional imaging in cancer and describe the use of selected quantitative imaging techniques for characterizing tumors that can be translated to clinical applications, particularly within the context of evaluating novel therapeutics and regimens. We also demonstrate how integrating the information from multiple imaging techniques may be used to provide a more comprehensive understanding of tumor status.

3. IMAGING BIOMARKERS AND MODALITIES

3.1. Proliferation assessment by FLT-PET

Noninvasive imaging approaches designed to longitudinally assess cellular proliferation offer considerable advantages over invasive approaches that rely upon serial biopsy. For this reason, investigation into suitable methodologies for imaging proliferation has been undertaken by a number of groups. Historically, several PET tracers that are precursors for DNA synthesis have been explored and include (11C) and (18F) labeled nucleosides and structural analogues (*1-3*). One of the most promising nucleoside-based imaging probes described thus far has been 3'-deoxy-3' (18F)-fluorothymidine, (18F)-FLT (*4-8*). Theoretically, (18F)-FLT and other nucleoside-based tracers may serve as surrogate markers of proliferation by reporting the activity of the thymidine salvage pathway, a cellular mechanism that utilizes uptake of deoxyribonucleosides from the extracellular environment to provide dividing cells with DNA precursors. Like other nucleosides such as thymidine, cytidine, and guanosine, (18F)-FLT is thought to be transported across the cell membrane by facilitated diffusion via low-affinity, non-concentrative nucleoside carrier proteins that are conserved across nearly all animal cells (*9*). Upon cellular internalization, (18F)-FLT is monophosphorylated in a reaction catalyzed by the cytosolic enzyme thymidine kinase 1 (TK1). Unlike thymidine, (18F)-FLT is not readily incorporated into DNA (*10*), yet phosphorylation to (18F)-FLT monophosphate results in intracellular trapping and subsequent accumulation. In many tissues, TK1 activity is regulated at transcriptional, translational, and post-translational levels (*11*) and activity tends to be closely correlated with the DNA synthesis phase of proliferating cells (typically late G1 through S). However, TK1 activity is typically diminished in quiescent, non-proliferating cells (*4, 12, 13*). Many pre-clinical and clinical studies have been published since the late 1990's exploring the utility of (18F)-FLT PET imaging as a quantitative metric to assess cellular proliferation in various species, tumor types, and organ sites (*4-8, 12*).

A fundamental understanding of the biological basis of FLT uptake limits the translatability of this tracer for broad scale clinical use in oncology. Currently, the relationship between (18F)-FLT uptake, TK1 biology, and cellular proliferation is not widely understood across various tumor types. Research published thus far has documented varying degrees of correlation between (18F)-FLT uptake and histological markers of proliferation such as Ki67 labeling indices. A rationale for this discrepancy can potentially be explained in a number of ways. As noted above, a central premise behind the use of (18F)-FLT uptake as a surrogate biomarker of proliferation is that dividing cells utilize thymidine salvage as a source of nucleoside precursors for DNA synthesis. While this premise holds true in certain situations, thymidine salvage is not a prerequisite for cell survival in replicating mammalian cells. In fact, thymidine salvage is a complementary route for providing cells with nucleosides with *de novo* synthesis of nucleosides being fully capable of providing all the DNA precursors needed for cell growth (*11*). Thus, (18F)-FLT uptake (if observed) in tumors relying predominately or completely on *de novo* nucleoside synthesis may poorly inform proliferation status compared with tumors that rely more heavily on thymidine salvage. At the present time, the prognostic and therapeutic implications for tumors that utilize *de novo* nucleoside synthesis versus thymidine salvage are not well understood within the field of cancer biology.

In addition to variations in cellular nucleoside utilization, differences in TK1 molecular biology likely contribute to a portion of the variability observed in (18F)-FLT PET imaging of tumors. A significant amount of research has been carried out towards understanding cellular regulation of TK1 expression and relevant biological factors that affect TK1 activity. Much of this research, however, has not yet translated directly into a broad understanding of (18F)-FLT uptake in tumors. At the genetic level, TK1 has been thoroughly characterized in normal cells; the gene is located on chromosome 17 and was cloned as early as 1983 (*14*). Despite the fact that TK1 activity tends to be highly regulated throughout the cell cycle and closely correlates with S-phase in normal cells, it has been shown that both overexpression of thymidine kinase mRNA (*15*) as well a defective p53 response (*16*) can lead to loss of cell cycle control of TK1 expression. Both of these conditions are common in tumor cells (*10*). Without compensation from TK1-specific proteolytic enzymes that degrade TK1 when expressed outside of S-phase, near-constitutive expression of TK1 could lead to greater intracellular concentrations of the enzyme and thus increased accumulation of (18F)-FLT in a given tumor.

Defects in cell cycle regulatory molecules can affect TK1 expression and activity in tumor cells. It has been shown that TK1 expression is negatively regulated via a p53/p21 dependent mechanism (*17*). Cyclin D, cyclin E, and p21 regulate the tumor suppressor retinoblastoma gene product (*Rb*), which when hypophosphorylated (*ppRb*) releases E2F transcription factors (*18-20*) to activate other downstream genes including TK1. Tumor cell defects in any of these cell cycle regulatory molecules are common

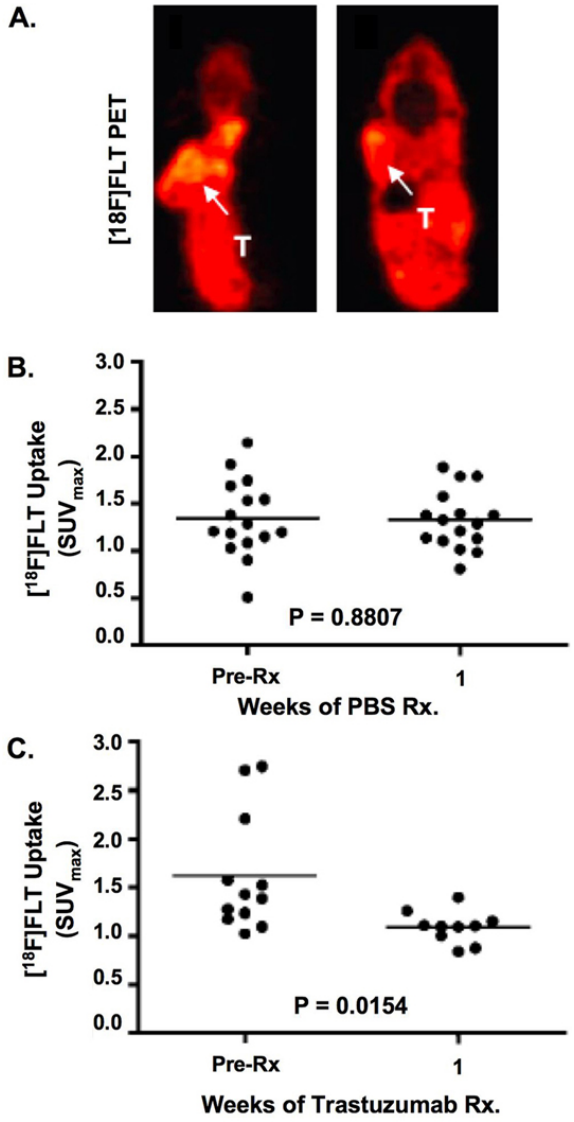

Figure 1. Assessment of (18F)FLT uptake in vehicle- and trastuzumab-treated BT474 human breast cancer xenografts. (18F)FLT-PET images of vehicle-treated (A) and trastuzumab-treated (B) BT474 tumor-bearing mice illustrating significantly reduced (18F)FLT uptake in the tumor of a trastuzumab treated mouse. No change in BT474 tumor (18F)FLT uptake was observed following vehicle treatment (C), yet a statistically significant decrease was observed across a cohort of trastuzumab-treated mice (D). All images and data shown were collected after 1 wk of vehicle or trastuzumab therapy. Reproduced with permission from (*23*), modified.

and lead to altered *Rb* activation and thus dysregulated E2F-dependant TK1 transcriptional activity. Interestingly, molecularly targeted therapies which may affect these regulatory molecules may also in turn affect TK1 expression in unexpected ways. For example, we recently reported that (18F)-FLT uptake does not appear to be an *in vivo* biomarker of response to EGF receptor blockade with cetuximab (mAb-C225) in DiFi human CRC xenografts (*21*). Derived from a rectal tumor arising in a patient with familial polyposis, DiFi cells express large amounts of EGF receptor (approximately 4M receptors/cell) and WT *KRAS* (*22*) and are therefore sensitive to cetuximab as monotherapy. Surprisingly, in our imaging studies we did not observe changes in (18F)-FLT uptake or Ki67 immunoreactivity following a multidose cetuximab regimen, despite observing significant levels of apoptosis and regression in responding tumors (*21*). However, in another recent study Shah *et al* explored several imaging metrics and found (18F)-FLT PET to be predictive of anti-HER2 therapy response (Figure 1) in a mouse model of HER2-positive breast cancer (*23*).

Interestingly, TK1 activity, but not necessarily TK1 expression, appears to be an ATP-dependant process (*11*). Functional TK1 is a tetrameric protein of approximately 100kDa; cDNA encodes a 25.5 kDa

monomer. In the absence of ATP, presumably an important cofactor for stabilization of the enzyme, monomeric and dimeric species tend to predominate. Seminal studies performed by Munch-Petersen and colleagues with purified human TK1 demonstrated improved TK1 activity in the presence of ATP (*24*). In these studies, ATP was shown to stabilize the TK1 tetramer and improve the binding affinity for substrate. More recently, Barthel and colleagues illustrated that (18F)-FLT uptake following chemotherapy (5-FU) more closely correlated with tumor cell ATP levels than TK1 levels (*25*). In these studies, prolonged tumor exposure to 5-FU led to reduced ATP levels yet increased TK1 expression. Presumably the translated enzyme was either inactive or destabilized due to reduced tumor ATP. It is plausible that this effect may be pronounced for treatments that directly affect ATP because in similar studies the same group did not observe an ATP dependency on (18F)-FLT uptake in tumors treated with a histone deacetylase (HDAC) inhibitor (*18*). However, these studies suggest that ATP levels can be a limiting factor and should be considered when utilizing (18F)-FLT as a biomarker of response.

Though not fully explored, nucleoside transporters may also play a role in affecting (18F)-FLT uptake in tumor cells. It has been demonstrated that nucleoside analogues with greater lipophilicity such as AZT may be able to circumvent nucleoside transporters (*26*). However, it has also been documented that cells with mutant nucleoside transporters have altered nucleoside uptake, which can affect intracellular deoxyribonucleotide pools (*11*).

In summary, though FLT PET imaging appears highly promising, we wish to emphasize that the relationship between (18F)-FLT uptake and proliferation in tumor cells is not entirely intuitive and additional basic research is needed to establish the role of this tracer in cancer imaging. As described, numerous factors routinely at play in cancer may significantly affect tracer uptake, which in turn may dictate how well cellular uptake of the tracer reflects proliferation. It is anticipated that future basic research studies will begin to elucidate important biological factors that dictate the degree to which (18F)-FLT PET is an informative biomarker of proliferation in cancer imaging.

3.2. Metabolism and PET

By far, the most commonly used PET tracer for clinical molecular imaging is (18F)2-fluoro-2-deoxy-D-glucose (FDG) in oncology. FDG-PET exploits the typically increased glucose metabolism of tumor tissues compared to surrounding normal tissues. FDG is transported into tumor cells via glucose transport proteins (such as GLUT1), which tend to be upregulated in tumor cells. Once FDG is internalized, the tracer is phosphorylated to FDG-6-phosphate by an enzyme known as hexokinase. Unlike glucose-6 phosphate, FDG-6-phosphate does not enter glycolysis due to the presence of fluorine substitution at the 2- position, and the tracer becomes metabolically trapped. Subsequent accumulation of FDG in metabolically active cells leads to imaging contrast. Some key drawbacks of FDG include non-specific accumulation in inflammation, as well as high background accumulation in highly metabolic tissues such as muscle and normal brain. The lack of specificity of FDG uptake does provide some anatomical references that can aid image interpretation, but the usefulness of this background signal has been rendered superfluous by the advent of hybrid PET/CT scanners in which the CT image provides more complete anatomical information.

The most frequently used measure of FDG accumulation is the Standardized Uptake Value (SUV). The SUV is a semi-quantitative measure that provides a means of comparing tumor uptake, for example, across individual scans and across patients by taking into account the amount of activity injected and the size of the subject. The SUV is the ratio of the activity concentration measured in the PET image and the injected dose divided by the subject's weight. Lean body mass or total body surface area is sometimes used instead of weight in calculating SUV, and these differences can complicate the comparison of scans from different sites. Using the mean SUV to characterize a tumor can be problematic, since it depends on how the tumor boundaries are delineated in selecting regions of interest (ROIs) and can be further complicated by tumor heterogeneity and the presence of necrotic regions. For this reason, the maximum SUV within the tumor ROI (SUV_{max}) is often used as the numeric measure of a tumor's glucose metabolism, despite the obvious statistical uncertainty of such a measure. While the use of SUV is an attempt to account for natural sources of variability in these imaging studies (injected dose and subject size), extreme care still is necessary in conducting such studies. First, studies must always be carried out with the same time delay between radiotracer injection and scanning. While there is no standard uptake period across institutions, scanning typically commences between forty and ninety minutes after FDG injection with sixty minutes being most common. Differences in the delay between injection and imaging affect not only the uptake at the target site but also the amount of background signal.

The distribution of FDG uptake also is highly dependent on such factors as blood glucose levels, body temperature, and amount of physical activity. While these factors have relatively little impact on the glucose metabolism of tumor tissues, they greatly affect the bioavailability of the radiotracer due to uptake in other regions of the body and, thereby, complicate estimation of FDG uptake from a single, static scan. Dynamic scans of radiotracer distribution accompanied by simplified kinetic measures, such as Patlak analysis of uptake rate, can be used to avoid some of these complications. More information can be obtained by carrying out full radiotracer kinetic modeling of dynamic image data. FDG uptake in such studies generally has been analyzed using a three-compartment (two tissue compartment) model, although some investigations of FDG uptake in skeletal muscle have utilized a four-compartment model in which delivery of FDG to the extracellular space, its transport to the intracellular space, and phosphorylation are treated separately. Despite the better quantitation that can be

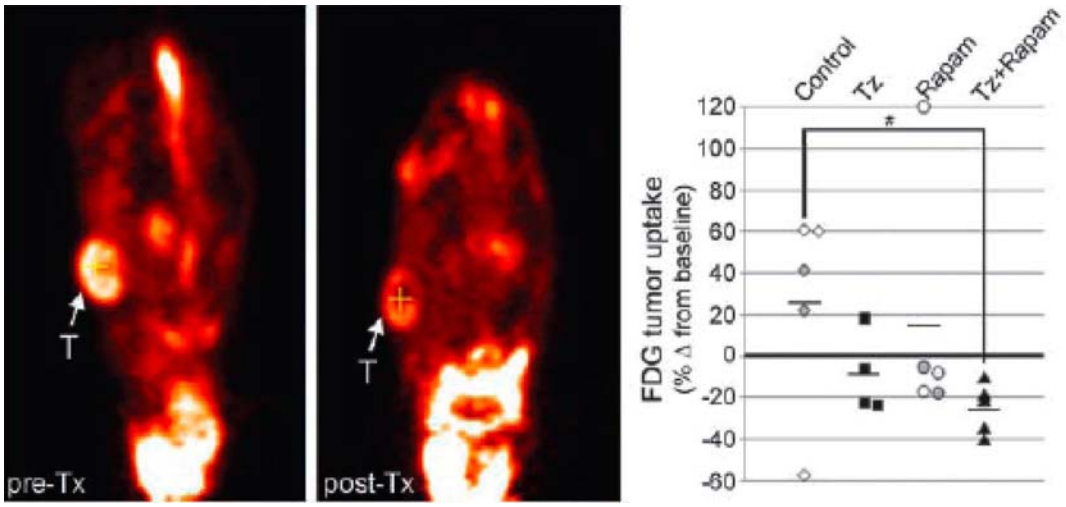

Figure 2. Rapamycin synergizes with trastuzumab to decrease tumor viability and glucose metabolism. Tumor-bearing mice were baseline imaged by positron emission tomography for (18F)FDG uptake, randomized to trastuzumab, rapamycin, or the combination (n = 5-6 per group) treatment on days 0, 2, 4, and 6, and reimaged on day 7 (n = 4-5 per group). Images from a representative mouse show (18F)FDG uptake pretreatment and post-treatment. Plot of the % change in (18F)FDG uptake at day 7 compared with baseline is shown (right). Gray diamonds/circles are indicative of two tumors within the same mouse. #, P = 0.0586, Mann-Whitney U test between treatment groups. Reproduced with permission from (*27*), modified.

obtained using these techniques, static scans are preferred in the clinical arena due to the greater subject throughput and the avoidance of blood sampling, which is needed to obtain the arterial input function for kinetic modeling. Meanwhile, full kinetic modeling in preclinical studies is complicated by the technical challenge of blood sampling in rodents. Image-derived arterial input functions are difficult to obtain in preclinical studies due to partial volume effects and accompanying spillover from myocardial uptake of FDG, but are the subject of active research.

Clinically, FDG-PET currently plays an important role in diagnosis and staging of several types of malignancies, particularly non-small-call lung cancer, colorectal cancer, melanoma, and lymphoma. Increasingly FDG-PET is also being used as a measure of response to therapy. Changes in tumor metabolism in response to therapeutic intervention as measured by FDG uptake have been shown to precede changes in tumor volume. For example, recent studies have employed FDG uptake as a readout of sensitivity to drug therapy in mouse models of HER2 positive breast cancer (Figure 2) (*27*) and non-small cell lung carcinoma (Figure 3) (*28*). In each study, drug therapy resulted in a marked decline of FDG uptake within the tumor volume within days of treatment commencement. Interestingly, with some forms of treatment such as tamoxifen therapy for breast cancer, an increase in FDG uptake 7-10 days after treatment has been observed in patients that respond positively to treatment, the so-called metabolic flare response. Such experience indicates that validation studies are required for each combination of tumor type and therapy to establish whether any link exists between treatment response and FDG-PET results. The new RECIST 1.1 criteria for the use of imaging in clinical trials include guidance on the use of FDG-PET.

As an alternative to assessing glucose metabolism with FDG, amino acid-based tracers can be used to measure protein metabolism. Tracers such as *O*-(2-18F-fluoroethyl)-L-tyrosine (18F)-FET have been used with particular success in brain tumors (*29*) because unlike FDG these agents have little uptake in normal brain tissues. Amino acid-based tracers typically show little uptake in inflammatory lesions, making them an attractive alternative to FDG in some cases as well. A drawback of amino acid tracers is rapid metabolism and attendant radioactive metabolites present in blood and tissues, which can confound interpretation of imaging data.

Cellular proliferation can also be estimated by measuring phospholipid metabolism with (11C)-choline. Choline imaging has been shown to be particularly useful in brain cancer and prostate cancer imaging where the increased activities of choline transporters and choline kinase are associated with increased cell membrane synthesis and proliferation. Similarly, (11C)-acetate, a precursor of fatty acid synthesis, can be used as a surrogate marker of metabolism and proliferation and has shown utility in prostate cancer and other diseases.

3.3. Angiogenesis and vascularity

Angiogenesis, or the formation and recruitment of new vasculature, is a highly orchestrated biological process that is primarily confined to wound healing and reproduction in healthy individuals. Dysregulated angiogenesis is a pathological condition and characteristic of a number of common diseases including diabetes, psoriasis, rheumatoid arthritis, and cancer (*30*). Angiogenesis plays a central role in the development and progression of tumors, as neovascularization is required to supply oxygen and nutrients to rapidly growing tumor cells and in turn facilitates the spread of metastases (*31*).

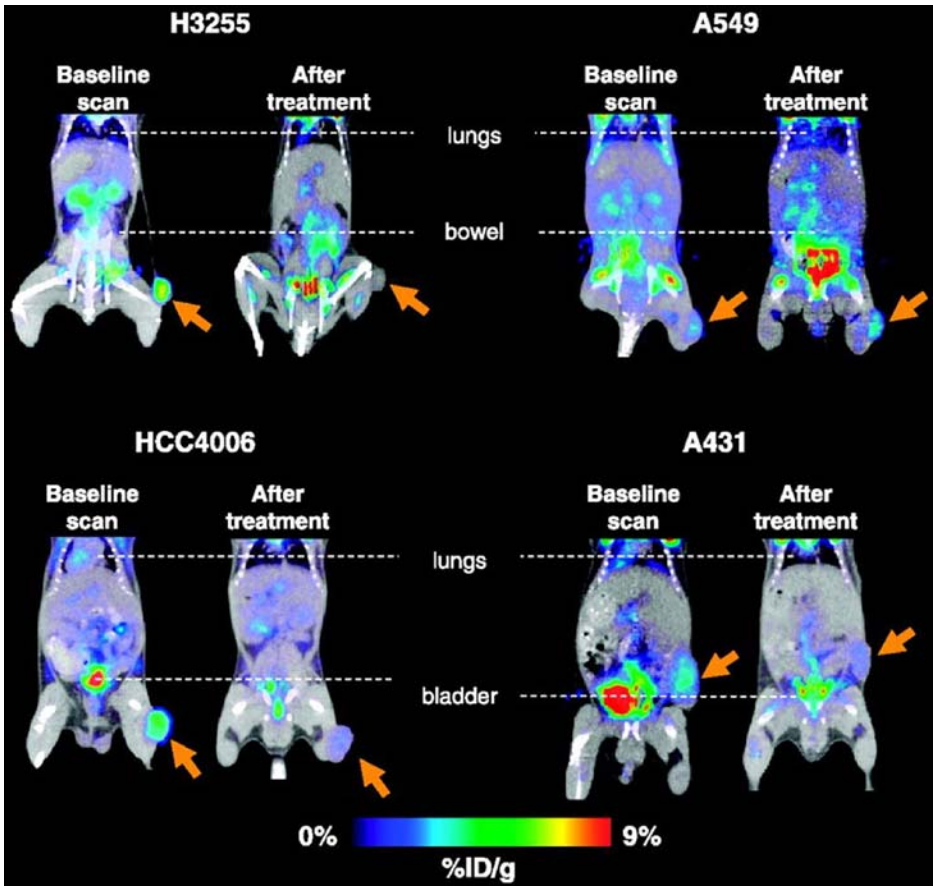

Figure 3. MicroPET/CT imaging of human tumor xenografts before and after gefitinib treatment. Tumor-bearing mice were subjected to a microPET/CT scan before (baseline scans) and after two oral doses of gefitinib (70mg/kg/d). Arrows denote the location of tumors. Reproduced with permission from (*28*), modified.

Objective, quantitative, non-invasive biomarkers of response to angiogenesis-directed therapies are increasingly important as the role angiogenesis plays in tumor initiation and progression is further appreciated. The development of improved tools that enable evaluation of novel therapeutic agents in preclinical animal models is essential. Within this setting, technologies are sought that facilitate rapid, cost-effective screening of large groups of animals (*32*). Imaging strategies commonly employed to assess angiogenesis include dynamic contrast enhanced magnetic resonance imaging (DCE-MRI) (*33*), ultrasound (*34*), computed tomography (*35*), and fluorescence perfusion imaging (*36*). In many cases, these techniques are well-established surrogates of angiogenesis and have proven utility (*37, 38*), but they are limited by their non-specific nature and low throughput (*39-41*). Since structural alterations resulting from inhibition of the vascular endothelial growth factor (VEGF) pathway lag the molecular event, early assessment of treatment response with these anatomical techniques is limited (*42*), underscoring a key advantage of our described molecular imaging approach.

Appreciation of the critical role angiogenesis plays in cancer progression has spurred development of a variety of angiogenesis-directed therapeutic agents, several of which are now clinically approved for use in various cancers (*43*). Tumor induced angiogenesis is predominately driven by paracrine VEGF signaling between tumor and/or stromal cells, which can secrete a variety of soluble VEGF ligands, and endothelial cells, which express tyrosine kinase VEGF receptors (*44-46*). Clinically employed approaches to inhibit VEGF signaling include therapeutic monoclonal antibodies (mAbs) such as bevacizumab (Avastin™) that aim to neutralize and sequester soluble VEGF ligands, as well as VEGF receptor-targeted small molecule tyrosine kinase inhibitors (TKIs) that inhibit receptor activation and signaling (*47-51*). While these and other angiogenesis-directed therapies appear promising and are rapidly entering into mainstream clinical use, a lack of objective, non-invasive biomarkers of response to this class of pharmaceuticals hinders the development and evaluation of these agents in the preclinical setting as well as the prediction of patients that are likely to benefit from these drugs clinically.

Non-invasive imaging modalities that directly assess molecular targets show considerable promise for monitoring numerous biological processes and therapeutic responses. The VEGF family of receptors is an attractive

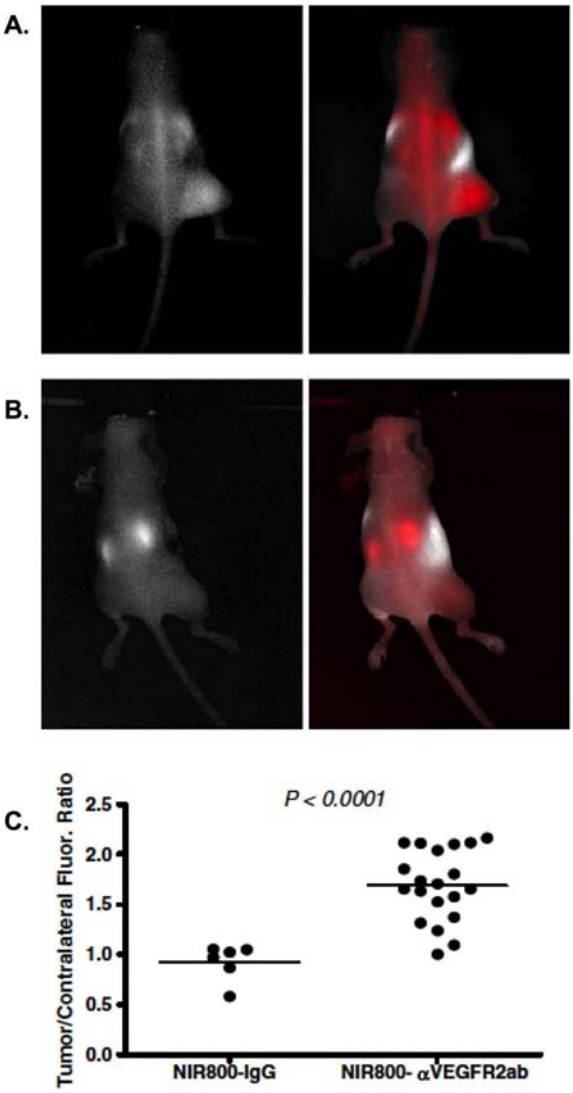

Figure 4. (A) representative fluorescence image of a mouse bearing a 4T1 xenograft tumor on the right hind limb. Image was collected 24 h after administration of NIR800-aVEGFR2ab demonstrating significant accumulation of the imaging probe within the tumor region. Single channel unmixed image of NIR800-aVEGFR2ab uptake (left) as well as multichannel fluorescence composite image of autofluorescence (white) and NIR800-aVEGFR2ab uptake (red) are shown (right). (B) representative fluorescence image of a mouse bearing a similar 4T1 xenograft tumor 24 h after administration of non-specific NIR800-IgG probe. Retention of the nonspecific probe was not observed within the tumor region. Single channel unmixed image of NIR800-IgG uptake (left) as well as composite image of autofluorescence (white) and NIR800-IgG (red) are shown (right). (C) quantified fluorescence intensity of the tumor region normalized to contralateral flank for mice injected with the NIR800-aVEGFR2ab probe (n=20) and the nonspecific NIR800-IgG probe (n=6). Reproduced with permission from (*64*).

class of imaging targets as they are primarily expressed on the surface of endothelial cells (*52*), which enables facile delivery of imaging compounds throughout the bloodstream. Molecular imaging of angiogenesis via VEGF receptor expression requires the use of sensitive imaging modalities because the receptors are predominately expressed on tumor-related vasculature, rather than tumor cells themselves, and therefore comprise only a minor fraction of a given tumor volume (*53*). Nuclear imaging methods, such as positron emission tomography (PET) and single photon emission computed tomography (SPECT), as well as optical imaging methods, such as fluorescence and bioluminescence techniques, possess the requisite sensitivity and are suitable modalities for studying angiogenesis (*32*). To this end, various VEGF receptor ligands have been labeled for PET/SPECT (*54-62*) and near-infrared (NIR) fluorescence imaging (*63*). One such example from our laboratory sought to image tumor angiogenesis in a mouse model of breast cancer by employing a NIR-labeled mAb based probe targeted to VEGFR2 (*64*). Retention of the targeted probe (Figure 4) was significantly increased over a control, untargeted probe, suggesting specific interaction with increased VEGF2 within the tumor region.

In many cases, imaging probes of this type have shown promise but may be limited by their reactivity with more than one VEGF receptor subtype, notably VEGFR1 and VEGFR2. VEGFR2 expression is most relevant to tumor angiogenesis, as VEGFR2 mediates the major angiogenic effects of VEGF. The significance of VEGFR1 is not fully understood in cancer but it appears that a possible role is to sequester VEGF (*65*). An additional drawback of ligand-based probes is that they can be prohibitively expensive to produce in sufficient quantity to support large, statistically meaningful studies in small animals or humans.

3.4. Cell death and cellularity

In normal cells, programmed cell death or apoptosis is a tightly regulated intracellular suicide program that is widely employed as a method for shedding redundant and/or dysfunctional cells. Cellular regulation of apoptosis proceeds via a complex cascade of intracellular signaling machinery that is conserved across a majority of animal cells. Specific molecular defects in apoptosis regulation are closely associated with numerous diseases including neurodegenerative disease and cancer. Considerable research has been undertaken to more closely understand apoptosis, particularly with respect to the adaptive mechanisms that many tumor cells utilize to maximize survival. Indeed, an impaired apoptosis program is a feature of many types of malignant tumor cells. Though the term ‘apoptosis’ itself was coined nearly 40 years ago by Kerr and colleagues (*66*) and an awareness of the general phenomenon has been known for many years prior to that (*67*), numerous biological factors affecting the molecular regulation of apoptosis still require further characterization at the basic science level.

Mitochondria are key players in the apoptotic program. In apoptosis, signaled release of cytochrome *c*,

which normally resides at the interface between the inner and outer mitochondrial membranes and serves to transfer electrons during oxidative phosphorylation, proceeds following depolarization of the outer membrane. Once released from mitochondria, cytosolic cytochrome *c* appears to initiate the apoptosis program. Release of cytochrome *c* occurs through specialized mitochondrial channels modulated by a large, complex family of regulatory molecules known as the Bcl-2 family of proteins. Twenty-four known Bcl-2-related proteins are encoded by the human genome; six of these proteins function to oppose apoptosis while the others promote apoptosis (*68*). Overall, a delicate balance between pro- and anti-apoptotic proteins governs the fate of individual cells. For example, the anti-apoptotic molecules Bcl-2 and Bcl-xL oppose apoptosis by facilitating the blockade of the channels responsible for release of cytochrome *c*. Conversely, by mechanisms that are not fully understood (*69*), pro-apoptotic Bcl-2 family members such as Bax, Bad, Bak, and Bid promote apoptosis by opening the channels and allowing cytochrome *c* to escape into the cytosol. Thus, mitochondrial release of cytochrome *c* is regulated in accordance with the relative intracellular levels of these pro- and anti-apoptotic proteins. Cancer cells commonly resist apoptosis by over-expressing pro-survival molecules such as Bcl-2 and Bcl-xL, or alternately, through inactivation of pro-apoptosis molecules such as Bax and Bad via phosphorylation and/or mutation.

Following cytochrome *c* release from mitochondria, much of the apoptosis program is controlled by an intracellular group of homologous cysteine proteases, or caspases. Of the dozen or so caspases thus far identified, at least two-thirds of these may play a role in regulation of apoptosis (*67, 70*). With exquisite selectivity that is dictated simply by the four residues amino-terminal to their activation site (*71*), caspases typically operate via site-specific cleavage of target proteins resulting in activation of pro-apoptotic targets or deactivation of pro-survival targets. When cytochrome *c* enters the cytoplasm, it associates with a molecule known as Apaf-1, forming a structure that has been termed the apoptosome, or 'wheel of death' (*68*). The resulting complex activates caspase 9, an initiator caspase, which in turn activates downstream executioner caspases such as 3, 6, and 7. The sequentially ordered activation of caspases, which begins with initiators triggering the onset of apoptosis signaling, and ends with executioners destroying critical components of the cell, forms the basis of the intracellular caspase signaling cascade. Caspase 3 is the final enzyme activated in the cascade and shortly after activation, breakdown of cellular proteins, cytoskeleton and nuclear contents follow. Subsequent activation of poly-ADP-ribose polymerase (PARP) facilitates the degradation of nuclear DNA into 50-300 kilobase pieces. The early execution phase of apoptosis is also closely associated with the redistribution and externalization of phosphotidyl serine (PS) to the cell surface, a process that is ATP and calcium ion-dependent (*72*). Interestingly, recognition of exposed PS has been shown to trigger the release of immunosuppressive cytokines that at least partially account for the lack of inflammation observed in response to apoptosis (*73*). Under the majority of normal circumstances, PS is restricted to the inner leaflet of the cell membrane lipid-bilayer.

Apoptosis can be initiated by multiple independent mechanisms in mammalian cells including an intrinsic, or stress activated pathway, and an extrinsic receptor-mediated pathway (*71*). The intrinsic pathway can be initiated by p53-dependant or p53-independent mechanisms and results in gene expression of pro-apoptotic molecules such as Bax. As previously noted, this results in the release of cytochrome *c* from the mitochondria, caspase activation, and cell death. Conversely, a receptor-mediated approach, termed the death receptor pathway, can be triggered externally through pro-apoptotic cell surface receptors such as FAS, DR4, and DR5 (*71*). Ligands for these receptors include tumor necrosis factor (TNF) proteins such as TNF-alpha, TRAIL, and Fas Ligand (FasL). Activation of death receptors through ligand engagement elicits a unique intracellular caspase cascade that eventually converges with the intrinsic apoptosis pathway downstream of caspase 8 activation. Beyond this point, the overall apoptotic response of the two pathways is similar.

Other non-apoptotic forms of cell-death are known and include such processes as necrosis, autophagy, and mitotic catastrophe. Apoptosis is unique when compared to these processes in important ways. Whereas apoptosis is a genetically regulated and concerted process, necrosis tends not to be. Additionally, apoptosis usually affects individual cells and does not affect neighbors, while necrosis tends to affect neighboring cells. Through release of toxic by-products, necrosis is detrimental to neighboring stroma (*68*). Inflammation is commonly observed with necrosis, but not in response to apoptosis. In contrast to both apoptosis and necrosis, autophagy is a recently described form of programmed cell death that appears to be activated in cells subjected to starvation stress (*74-76*). Cells undergoing autophagy employ cytoplasmic lysosomes to digest their own intracellular organelles, with many of the resulting chemical species being recyclable for later consumption. Like autophagy, mitotic catastrophe is another interesting form of cell death. Though not as fully characterized, mitotic catastrophe appears to occur during mitosis and results from a combination of deficient cell-cycle checkpoints and prior cellular damage (*77*).

Significant efforts have gone into the development of non-invasive imaging methods to longitudinally assess apoptosis. Many of these efforts have focused on the use of Annexin-V, an endogenous 36 kDa human protein that binds PS with nanomolar affinity, as a PS targeted carrier. Numerous clinical studies have demonstrated promising results with SPECT imaging of ^{99m}Tc-labeled Annexin-V to assess apoptosis in patients with cancer (*78-83*), myocardial infarction (*84, 85*), ischemic preconditioning (*86*), vulnerable atherosclerotic plaques (*87*), acute stroke imaging (*88, 89*), and Alzheimer's dementia (*90*). Additionally, fluorophore-labeled versions of Annexin-V have been utilized for flow cytometry and for imaging response to therapy in animal models (*91, 92*). For example, we recently reported use of

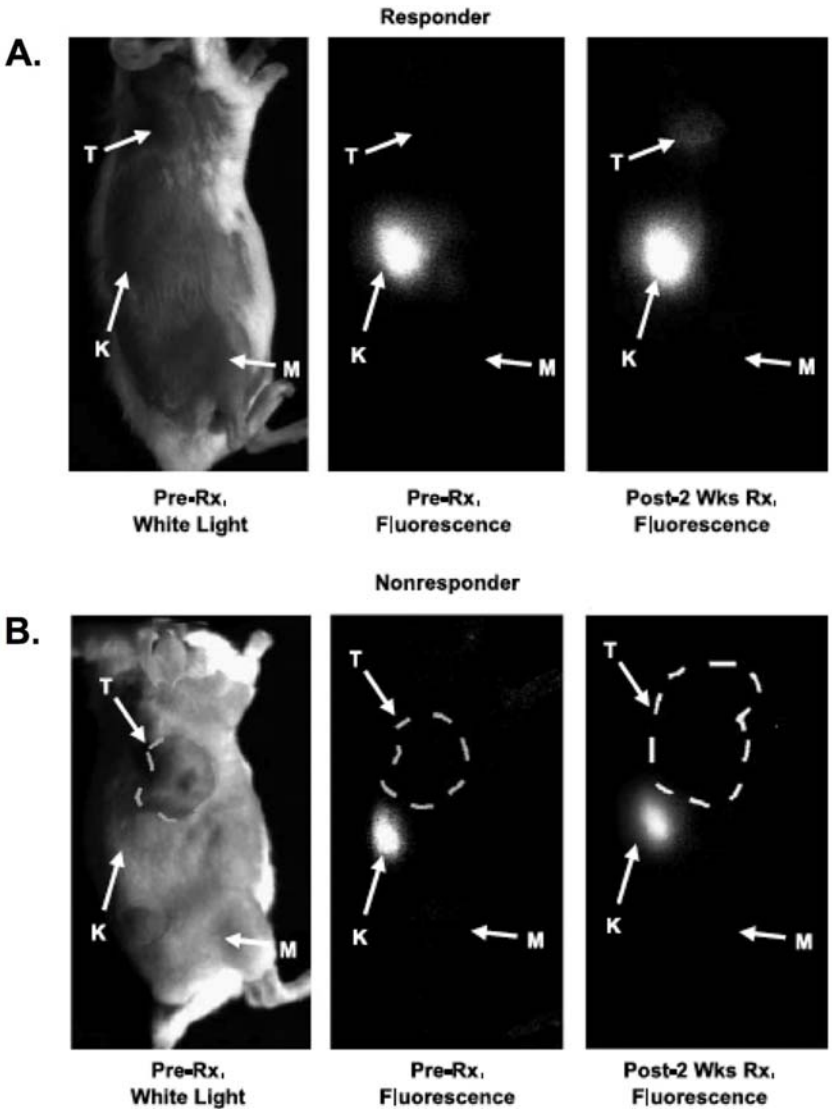

Figure 5. Accumulation of NIR700-AnnexinV is enhanced in MMTV/HER2 tumors responding to trastuzumab. NIR700-AnnexinV was administered i.v., and mice were serially imaged up to 44 h before and after treatments with trastuzumab or vehicle (PBS). Representative images from responding (A) and nonresponding (B) MMTV/HER2 tumor-bearing mice (24h images shown). Significant accumulation of NIR700-AnnexinV was observed within the responsive tumor after 2 wk of trastuzumab treatment (A), whereas the nonresponsive tumor does not show significant NIR700-AnnexinV uptake (B). T, tumor; K, kidney; M, reference muscle. Reproduced with permission from (*23*).

a near-infrared dye labeled Annexin-V derivative to assess response to cetuximab and trastuzumab therapy in mouse models of colorectal (*21*) and breast (*23*) cancer. In these studies, we observed significant accumulation of Annexin-V in the tumors of responding, but not non-responding, cohorts (Figure 5).

Though previous use of Annexin-V to assess apoptosis has yielded promising results, additional studies are necessary to characterize and validate factors that affect Annexin-V uptake in tumor cells. It is generally accepted that externalization of PS is closely associated with apoptosis, yet emerging evidence is now suggesting that this may not always be true. Surprisingly, there is no direct evidence that PS externalization is dependent upon cytochrome *c* release, caspase activation, and/or DNA fragmentation (*93*). Additionally, transient PS expression has been reported in viable, non-apoptotic cells (*94, 95*), suggesting the existence of PS externalization mechanisms unrelated to apoptosis. Recently it was documented that PS externalization can reversibly occur through a mechanism independent of cytochrome *c* release, caspase activation, and DNA fragmentation (*93*). The same study suggested an important role for sustained concentrations of cytosolic Ca^{2+} and inactivation of translocase for translocation of PS (*93*). Overall, these studies suggest that substantial validation of apoptosis imaging metrics must be conducted within appropriate, disease-specific, therapeutic contexts.

Novel strategies to image apoptosis have been suggested and are being evaluated. Given that significant membrane reorganization occurs during the apoptosis process, one promising class of imaging agents include small molecules that are selectively permeable to apoptotic cell membranes. One such compound, (18F)-ML-10, has recently shown promise as apoptosis imaging probe in cerebral stroke imaging *in vivo (96)*. Additionally, both small molecule and peptide-based probes targeting caspase 3/7 expression are also being developed and have shown some promise as *in vivo* imaging probes (*97*).

Beyond molecular imaging of specific cellular proteins or by-products, tissue cellularity can be assessed on a more macroscopic level. The thermally induced behavior of molecules moving in a random pattern is referred to as self-diffusion or Brownian motion. The rate of diffusion in tissues is lower than in free solution and is described by an apparent diffusion coefficient (ADC), which largely depends on the number, permeabilities and separation of barriers that a diffusing water molecule encounters. Magnetic resonance imaging (MRI) methods have been developed to map the ADC, and in well-controlled situations the variations in ADC have been shown to correlate inversely with tissue cellularity (*98*). ADC values in tissues tend to be significantly lower than that those found in free solution due to the fact that water migration is hindered by passage through membranes and molecular interaction with a variety of cellular milieu such as proteins and organelles. For diagnosis of pathological conditions such as ischemic stroke (*99, 100*), affected tissues have been shown to produce significantly different ADC values compared to healthy tissues. Additionally, because of the increased cellularity commonly observed in solid tumors, ADC values of tumor tissue tend to be significantly lower than surrounding normal tissues. This phenomenon forms that basis of ADC-MRI as a potential cancer imaging biomarker.

Despite ever increasing utilization of diffusion MRI for oncology applications, there is a critical need for improved understanding and validation of the cellular and molecular factors that affect water diffusion rates in tissues. Recent efforts to utilize pre-treatment ADC values as a prognostic biomarker in human rectal cancer (*101*) and colorectal cancer liver metastases (*102, 103*), as well as in mouse models of colorectal cancer (*104*) and breast cancer (*105*), have shown mixed results. Generally in the human studies reported, higher pre-treatment ADC values tend to correlate with poorer response to therapy and prognosis (*101-103*). For example, in a recent study characterizing hepatic metastases with ADC-MRI, thirty-eight responding and forty-nine non-responding lesions were evaluated in patients with confirmed metastases originating from gastrointestinal cancers (*102*). In these patients, the mean pre-therapy ADC for non-responding lesions was found to be significantly higher than that of non-responding lesions. Similarly, in a study reporting a smaller group of patients presenting with colorectal hepatic metastases, Koh *et al* found that higher pre-treatment ADC values were predictive of poor response to chemotherapy (*103*). Interestingly, recent work employing HT-29 colorectal cancer xenografts grown in athymic nude mice found no correlation between pre-treatment ADC values and response to chemotherapy (*104*). Combined with human imaging studies, these results suggest that additional animal modeling studies are warranted to more completely understand the prognostic value of pre-treatment ADC values. We wish to emphasize that while the studies conducted to date have generally considered the prognostic value of ADC imaging with respect to cytotoxic or radiation therapies, we are unaware of any studies that have thoroughly considered the prognostic value of ADC imaging within the context of more novel molecularly targeted therapies as proposed here. Additionally, further preclinical modeling efforts must include not only xenograft models as are commonly employed, but must also increasingly emphasize mouse models that place the tumor within a more appropriate microenvironmental context.

Towards quantitative assessment of therapeutic regimens, early responses to various interventions have correlated with increasing ADC values in many studies. Representative reports illustrating increased ADC in correlation with ultimate tumor response following early intervention include studies involving human brain tumors (*106*), brain tumor animal models (*107*), prostate metastases to bone (*108*), human breast tumors (*109*), mouse models of breast cancer (*105, 110*), primary rectal tumors (*101*), CRC hepatic metastasis (*102, 103*), and mouse models of CRC (*104*). Importantly, the vast majority of these studies have been performed in combination with either cytotoxic drugs and/or chemoradiation, and thus ADC response to molecularly targeted therapy is not well established. However, a recent example from our laboratory examined the ADC response of a mouse CRC model treated with a targeted cetuximab therapy (Figure 6, Manning *et al*, unpublished data). In this study, a significant increase in the average ADC value was observed across the tumor volume in response to cetuximab treatment, consistent with measures in a number of other tumor models. Generally, the observed increase in ADC values following therapy appears to be a phenomenon which can stem from a number of cell death mechanisms including apoptosis (*105*), lytic necrosis, autophagy, and/or mitotic catastrophe (*110*). Because water within tumor cells is in a restricted environment relative to extracellular water, loss of cell membrane integrity and cellular density resulting from any or all of these cell death mechanisms could play a role in the observed changes in ADC following therapy. Additionally, cell death responses can be intervention and/or tumor-type dependent. Recent studies in preclinical models have illustrated observable ADC changes following treatments resulting in primarily apoptosis (*105*) as well as preclinical models where non-apoptotic cell death mechanisms predominate (*110*). Since many tumors can rapidly outgrow their vascular and nutrient supply, extreme metabolic stress as well as drastic changes in hypoxia and pH can induce progressively substantial central necrosis. Occurring in absence of treatment and unregulated by genetic control, necrosis can occur rapidly and is typically accompanied by significant inflammation and marked cell lysis. It is noteworthy that

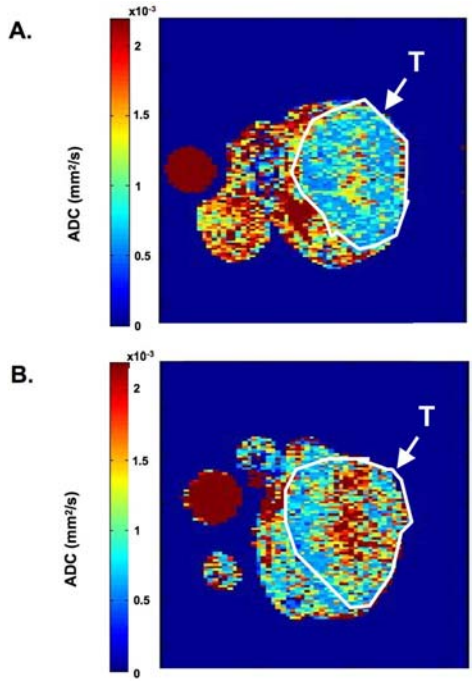

Figure 6. ADC maps before (A) and after (B) treatment of DiFi xenograft tumor with C225. ADC values in tumor are lower than surrounding normal tissues prior to C225 treatment; "T" = tumor. Weighted mean ADC pre-treatment = 9.93e-04 mm^2/s. Following C225, increased ADC is observed in the tumor. Weighted mean ADC post-treatment = 1.2e-03 mm^2/s.

the process of necrosis is vastly different than that of apoptosis, but these two processes can occur in concert at times. Additionally, a non-apoptosis form of programmed cell death, known as autophagy, has been noted and is distinct from apoptosis (*74-76*) and necrosis. In general, roles for autophagy in cancer are emerging, and under normal circumstances it may play a significant role in the elimination of cells that suffer from nutrient starvation as well as in the prevention of tumorigenesis (*74, 75*). Establishing the specific contribution of various cell death mechanisms such as apoptosis, autophagy, and/or necrosis within the contexts of particular tumor types and therapeutic strategies is of great importance towards the basic validation of ADC-MRI. Ultimately, sorting out the range of specific cellular and molecular responses that give rise to changes in ADC within well characterized preclinical models may also benefit the development of novel diffusion MRI techniques such as the novel OGSE methods developed at Vanderbilt University (*111*).

3.5. Receptor-targeted probes

A key area of molecular imaging research has historically been and continues to be based on imaging agents that bind to cell surface receptors with high specificity. PET imaging, with its high sensitivity and quantitative capability, is a particularly powerful tool for such studies, especially those performed in the brain. Neuroreceptor imaging plays an important role in the diagnosis and study of neurodegenerative disorders such as Parkinson's disease. Another major use of neuroreceptor imaging involves quantitative occupancy studies central to drug discovery for the treatment of psychiatric disorders. Additionally, many studies are conducted to evaluate the effects of drugs, including drugs of abuse such as methamphetamine and cocaine, on brain function (*112*). One of the more common targets of such neuroreceptor imaging studies has been the dopaminergic system, and numerous tracers such as (18F)-Fallypride (*113*) and (11C)-raclopride (*114*) exist for this purpose.

Molecular imaging of receptor expression is also important in oncology. In breast cancer, (18F)-Fluoroestrodiol (FES) has been shown to predict those patients who will respond to endocrine therapy (*115, 116*). Additionally, imaging probes targeting endothelial growth factor receptor (EGFR) and HER-2 have been prepared and shown to have potential for the evaluation of receptor status in tumors (*21, 117*). (111In)-DTPA-D-Phe-octreotide is a routine clinical tool for evaluation of somatostatin receptor in neuroendocrine tumors, yet PET analogs bearing either 68Ga or 64Cu are also being evaluated to extend somatostatin receptor imaging to PET where sensitivity is somewhat better.

Another important receptor in cancer imaging, EGFR, is a large transmembrane protein family that consists of 4 distinct types: HER1/erbB1, HER2/erbB2, HER3/erbB3 and HER4/erbB4 (*118, 119*). All 4 receptors exhibit significant homology in their extracellular binding domain, as well as a transmembrane domain, and an intracellular protein tyrosine kinase domain. HER3/erbB3 stands out with its lack of intracellular kinase domain. Being a large family, these receptors can form dynamic heterogeneous or homogenous complexes that govern the most vital signaling events in cell growth and proliferation (*120*). Upon distinct ligand binding, these receptors can activate key signaling pathways such as the mitogen activated protein kinase (MAPK) and phosphoinositide 3-kinase (PI3K) pathways. Overexpression (*121*), upregulation (*122, 123*) and mutations (*124*) in EGFR can cause abnormal cell proliferation and tumorigenesis. Receptor overexpression induces constitutive autocrine activation by its upregulated ligand such as transforming growth factor receptor alpha (TGFalpha) (*125*). Due to its importance in cancer initiation and progression, the EGFR receptor family has been the main focus of molecular targeted therapies in recent years.

There are several EGFR targeted therapies currently available in the clinic including mAbs, reversible and irreversible small TKIs, and antisense oligonucleotides (*126*). The chimeric human-murine mAb cetuximab has been shown to bind and inhibit EGFR regulated pathway activation (*127*), induce apoptosis (*128*), block angiogenesis in dose-dependent manner (*129*) and inhibit tumor growth and metastasis by downregulating VEGF, interleukin-8 (IL-8), and basic fibroblast growth factor (bFGF) (*130*). As a small molecule inhibitor example, gefitinib (Iressa) is reported to inhibit EGFR and cause tumor growth regression in both *in vitro* and human tumor xenografts (*131*). As a result of its clinical importance,

development of non-invasive EGFR imaging modalities will provide vital information regarding tumor status and response to therapy.

4. SUMMARY AND PERSPECTIVE

Various imaging measures can depict specific intracellular, extracellular, and structural changes in tumors following treatment and can therefore potentially be used as biomarkers clinically and in research. Molecular changes detected by nuclear imaging techniques may be the most sensitive and specific (e.g. for assessing whether a "target" is affected by a drug), but less tumor-specific physiological assessments (e.g. metabolism, cell density) "downstream" of the primary events may also provide reliable insights into the overall therapeutic response and be more practical for translation into clinical practice. In the future, hybrid scanners capable of simultaneously acquiring multi-modal images beyond the new universal PET/CT, and thus multiple biomarkers simultaneously such as ADC-MRI/PET, will likely be available, but reliable and robust image co-registration algorithms will also permit integration of the information from multiple measurements, increasing the information available to investigators in synergistic fashion. Although molecular imaging appears to provide tools well suited to personalized medicine, there remains some uncertainty as to which molecular imaging agents and techniques may become a standard part of clinical practice. In addition to the scientific aspect of the question, regulatory and reimbursement issues also are important factors influencing the evolution of molecular imaging. A framework through which novel imaging metrics and molecular imaging agents themselves find a path to FDA approval is currently an important topic for discussion.

5. REFERENCES

1. Reinhardt, M. J., K. Kubota, S. Yamada, R. Iwata & H. Yaegashi: Assessment of cancer recurrence in residual tumors after fractionated radiotherapy: a comparison of fluorodeoxyglucose, L-methionine and thymidine. *J Nucl Med*, 38, 280-7 (1997)

2. Shields, A. F., D. Mankoff, M. M. Graham, M. Zheng, S. M. Kozawa, J. M. Link & K. A. Krohn: Analysis of 2-carbon-11-thymidine blood metabolites in PET imaging. *J Nucl Med*, 37, 290-6 (1996)

3. Shields, A. F., D. A. Mankoff, J. M. Link, M. M. Graham, J. F. Eary, S. M. Kozawa, M. Zheng, B. Lewellen, T. K. Lewellen, J. R. Grierson & K. A. Krohn: Carbon-11-thymidine and FDG to measure therapy response. *J Nucl Med*, 39, 1757-62 (1998)

4. Chen, W., T. Cloughesy, N. Kamdar, N. Satyamurthy, M. Bergsneider, L. Liau, P. Mischel, J. Czernin, M. E. Phelps & D. H. Silverman: Imaging proliferation in brain tumors with 18F-FLT PET: comparison with 18F-FDG. *J Nucl Med*, 46, 945-52 (2005)

5. Choi, S. J., J. S. Kim, J. H. Kim, S. J. Oh, J. G. Lee, C. J. Kim, Y. S. Ra, J. S. Yeo, J. S. Ryu & D. H. Moon: (18F)3'-deoxy-3'-fluorothymidine PET for the diagnosis and grading of brain tumors. *Eur J Nucl Med Mol Imaging*, 32, 653-9 (2005)

6. Cobben, D. C., P. H. Elsinga, A. van Waarde & P. L. Jager: Correspondence re: H. Barthel *et al.*, 3'-deoxy-3'- ((18)F)fluorothymidine as a new marker for monitoring tumor response to antiproliferative therapy *in vivo* with positron emission tomography. Cancer Res., 63: 3791-3798, 2003. *Cancer Res*, 63, 8558-9; author reply 8560 (2003)

7. Dittmann, H., B. M. Dohmen, F. Paulsen, K. Eichhorn, S. M. Eschmann, M. Horger, M. Wehrmann, H. J. Machulla & R. Bares: (18F)FLT PET for diagnosis and staging of thoracic tumours. *Eur J Nucl Med Mol Imaging*, 30, 1407-12 (2003)

8. Grierson, J. R., J. L. Schwartz, M. Muzi, R. Jordan & K. A. Krohn: Metabolism of 3'-deoxy-3'- (F-18)fluorothymidine in proliferating A549 cells: validations for positron emission tomography. *Nucl Med Biol*, 31, 829-37 (2004)

9. Plagemann, P. G., R. M. Wohlhueter & C. Woffendin: Nucleoside and nucleobase transport in animal cells. *Biochim Biophys Acta*, 947, 405-43 (1988)

10. Toyohara, J., A. Waki, S. Takamatsu, Y. Yonekura, Y. Magata & Y. Fujibayashi: Basis of FLT as a cell proliferation marker: comparative uptake studies with (3H)thymidine and (3H)arabinothymidine, and cell-analysis in 22 asynchronously growing tumor cell lines. *Nucl Med Biol*, 29, 281-7 (2002)

11. Arner, E. S. & S. Eriksson: Mammalian deoxyribonucleoside kinases. *Pharmacol Ther*, 67, 155-86 (1995)

12. Wagner, M., U. Seitz, A. Buck, B. Neumaier, S. Schultheiss, M. Bangerter, M. Bommer, F. Leithauser, E. Wawra, G. Munzert & S. N. Reske: 3'- (18F)fluoro-3'-deoxythymidine ((18F)-FLT) as positron emission tomography tracer for imaging proliferation in a murine B-Cell lymphoma model and in the human disease. *Cancer Res*, 63, 2681-7 (2003)

13. Waldherr, C., I. K. Mellinghoff, C. Tran, B. S. Halpern, N. Rozengurt, A. Safaei, W. A. Weber, D. Stout, N. Satyamurthy, J. Barrio, M. E. Phelps, D. H. Silverman, C. L. Sawyers & J. Czernin: Monitoring antiproliferative responses to kinase inhibitor therapy in mice with 3'-deoxy-3'-18F-fluorothymidine PET. *J Nucl Med*, 46, 114-20 (2005)

14. Bradshaw, H. D., Jr.: Molecular cloning and cell cycle-specific regulation of a functional human thymidine kinase gene. *Proc Natl Acad Sci U S A*, 80, 5588-91 (1983)

15. Mikulits, W., M. Hengstschlager, T. Sauer, E. Wintersberger & E. W. Mullner: Overexpression of thymidine kinase mRNA eliminates cell cycle regulation of thymidine kinase enzyme activity. *J Biol Chem*, 271, 853-60 (1996)

16. Schwartz, J. L., Y. Tamura, R. Jordan, J. R. Grierson & K. A. Krohn: Effect of p53 activation on cell growth, thymidine kinase-1 activity, and 3'-deoxy-3'fluorothymidine uptake. *Nucl Med Biol*, 31, 419-23 (2004)

17. de Toledo, S. M., E. I. Azzam, P. Keng, S. Laffrenier & J. B. Little: Regulation by ionizing radiation of CDC2, cyclin A, cyclin B, thymidine kinase, topoisomerase IIalpha, and RAD51 expression in normal human diploid fibroblasts is dependent on p53/p21Waf1. *Cell Growth Differ*, 9, 887-96 (1998)

18. Leyton, J., J. P. Alao, M. Da Costa, A. V. Stavropoulou, J. R. Latigo, M. Perumal, R. Pillai, Q. He, P. Atadja, E. W. Lam, P. Workman, D. M. Vigushin & E. O. Aboagye: *In vivo* biological activity of the histone deacetylase inhibitor LAQ824 is detectable with 3'-deoxy-3'- (18F)fluorothymidine positron emission tomography. *Cancer Res*, 66, 7621-9 (2006)

19. McCabe, M. T., O. J. Azih & M. L. Day: pRb-Independent growth arrest and transcriptional regulation of E2F target genes. *Neoplasia*, 7, 141-51 (2005)

20. Yu, J. T., R. G. Foster & D. C. Dean: Transcriptional repression by RB-E2F and regulation of anchorage-independent survival. *Mol Cell Biol*, 21, 3325-35 (2001)

21. Manning, H. C., N. B. Merchant, A. C. Foutch, J. M. Virostko, S. K. Wyatt, C. Shah, E. T. McKinley, J. Xie, N. J. Mutic, M. K. Washington, B. LaFleur, M. N. Tantawy, T. E. Peterson, M. S. Ansari, R. M. Baldwin, M. L. Rothenberg, D. J. Bornhop, J. C. Gore & R. J. Coffey: Molecular imaging of therapeutic response to epidermal growth factor receptor blockade in colorectal cancer. *Clin Cancer Res*, 14, 7413-22 (2008)

22. Olive, M., S. Untawale, R. J. Coffey, M. J. Siciliano, D. M. Wildrick, H. Fritsche, S. Pathak, L. M. Cherry, M. Blick, P. Lointier & *et al.*: Characterization of the DiFi rectal carcinoma cell line derived from a familial adenomatous polyposis patient. *In vitro Cell Dev Biol*, 29A, 239-48 (1993)

23. Shah, C., T. W. Miller, S. K. Wyatt, E. T. McKinley, M. G. Olivares, V. Sanchez, D. D. Nolting, J. R. Buck, P. Zhao, M. S. Ansari, R. M. Baldwin, J. C. Gore, R. Schiff, C. L. Arteaga & H. C. Manning: Imaging biomarkers predict response to anti-HER2 (ErbB2) therapy in preclinical models of breast cancer. *Clin Cancer Res*, 15, 4712-21 (2009)

24. Munch-Petersen, B., G. Tyrsted & L. Cloos: Reversible ATP-dependent transition between two forms of human cytosolic thymidine kinase with different enzymatic properties. *J Biol Chem*, 268, 15621-5 (1993)

25. Barthel, H., M. C. Cleij, D. R. Collingridge, O. C. Hutchinson, S. Osman, Q. He, S. K. Luthra, F. Brady, P. M. Price & E. O. Aboagye: 3'-deoxy-3'-(18F)fluorothymidine as a new marker for monitoring tumor response to antiproliferative therapy *in vivo* with positron emission tomography. *Cancer Res*, 63, 3791-8 (2003)

26. Plagemann, P. G. & C. Woffendin: Permeation and salvage of dideoxyadenosine in mammalian cells. *Mol Pharmacol*, 36, 185-92 (1989)

27. Miller, T. W., J. T. Forbes, C. Shah, S. K. Wyatt, H. C. Manning, M. G. Olivares, V. Sanchez, T. C. Dugger, N. de Matos Granja, A. Narasanna, R. S. Cook, J. P. Kennedy, C. W. Lindsley & C. L. Arteaga: Inhibition of mammalian target of rapamycin is required for optimal antitumor effect of HER2 inhibitors against HER2-overexpressing cancer cells. *Clin Cancer Res*, 15, 7266-76 (2009)

28. Su, H., C. Bodenstein, R. A. Dumont, Y. Seimbille, S. Dubinett, M. E. Phelps, H. Herschman, J. Czernin & W. Weber: Monitoring tumor glucose utilization by positron emission tomography for the prediction of treatment response to epidermal growth factor receptor kinase inhibitors. *Clin Cancer Res*, 12, 5659-67 (2006)

29. Stadlbauer, A., O. Prante, C. Nimsky, E. Salomonowitz, M. Buchfelder, T. Kuwert, R. Linke & O. Ganslandt: Metabolic imaging of cerebral gliomas: spatial correlation of changes in O- (2-18F-fluoroethyl)-L-tyrosine PET and proton magnetic resonance spectroscopic imaging. *J Nucl Med*, 49, 721-9 (2008)

30. Folkman, J.: Angiogenesis in cancer, vascular, rheumatoid and other disease. *Nat Med*, 1, 27-31 (1995)

31. Folkman, J., K. Watson, D. Ingber & D. Hanahan: Induction of angiogenesis during the transition from hyperplasia to neoplasia. *Nature*, 339, 58-61 (1989)

32. Massoud, T. F. & S. S. Gambhir: Molecular imaging in living subjects: seeing fundamental biological processes in a new light. *Genes Dev*, 17, 545-80 (2003)

33. Tofts, P. S.: Modeling tracer kinetics in dynamic Gd-DTPA MR imaging. *J Magn Reson Imaging*, 7, 91-101 (1997)

34. Ferrara, K. W., C. R. Merritt, P. N. Burns, F. S. Foster, R. F. Mattrey & S. A. Wickline: Evaluation of tumor angiogenesis with US: imaging, Doppler, and contrast agents. *Acad Radiol*, 7, 824-39 (2000)

35. Numaguchi, Y., T. Kishikawa, M. Fukui, K. Sawada, K. Kitamura, K. Matsuura & W. J. Russell: Prolonged injection angiography for diagnosing intracranial cavernous hemangiomas. *Radiology*, 131, 137-8 (1979)

36. Ntziachristos, V., A. G. Yodh, M. Schnall & B. Chance: Concurrent MRI and diffuse optical tomography of breast after indocyanine green enhancement. *Proc Natl Acad Sci U S A*, 97, 2767-72 (2000)

37. Drevs, J., I. Hofmann, H. Hugenschmidt, C. Wittig, H. Madjar, M. Muller, J. Wood, G. Martiny-Baron, C. Unger & D. Marme: Effects of PTK787/ZK 222584, a specific inhibitor of vascular endothelial growth factor receptor tyrosine kinases, on primary tumor, metastasis, vessel density, and blood flow in a murine renal cell carcinoma model. *Cancer Res*, 60, 4819-24 (2000)

38. Marzola, P., A. Degrassi, L. Calderan, P. Farace, E. Nicolato, C. Crescimanno, M. Sandri, A. Giusti, E. Pesenti, A. Terron, A. Sbarbati & F. Osculati: Early antiangiogenic activity of SU11248 evaluated *in vivo* by dynamic contrast-enhanced magnetic resonance imaging in an experimental model of colon carcinoma. *Clin Cancer Res*, 11, 5827-32 (2005)

39. Forsberg, F., A. P. Dicker, M. L. Thakur, N. M. Rawool, J. B. Liu, W. T. Shi & L. N. Nazarian: Comparing contrast-enhanced ultrasound to immunohistochemical markers of angiogenesis in a human melanoma xenograft model: preliminary results. *Ultrasound Med Biol*, 28, 445-51 (2002)

40. Knopp, M. V., E. Weiss, H. P. Sinn, J. Mattern, H. Junkermann, J. Radeleff, A. Magener, G. Brix, S. Delorme, I. Zuna & G. van Kaick: Pathophysiologic basis of contrast enhancement in breast tumors. *J Magn Reson Imaging*, 10, 260-6 (1999)

41. Su, M. Y., Y. C. Cheung, J. P. Fruehauf, H. Yu, O. Nalcioglu, E. Mechetner, A. Kyshtoobayeva, S. C. Chen, S. Hsueh, C. E. McLaren & Y. L. Wan: Correlation of dynamic contrast enhancement MRI parameters with microvessel density and VEGF for assessment of angiogenesis in breast cancer. *J Magn Reson Imaging*, 18, 467-77 (2003)

42. Ocak, I., P. Baluk, T. Barrett, D. M. McDonald & P. Choyke: The biologic basis of *in vivo* angiogenesis imaging. *Front Biosci*, 12, 3601-16 (2007)

43. Folkman, J.: Tumor angiogenesis: therapeutic implications. *N Engl J Med*, 285, 1182-6 (1971)

44. Ferrara, N. & W. J. Henzel: Pituitary follicular cells secrete a novel heparin-binding growth factor specific for vascular endothelial cells. *Biochem Biophys Res Commun*, 161, 851-8 (1989)

45. Folkman, J., E. Merler, C. Abernathy & G. Williams: Isolation of a tumor factor responsible for angiogenesis. *J Exp Med*, 133, 275-88 (1971)

46. Leung, D. W., G. Cachianes, W. J. Kuang, D. V. Goeddel & N. Ferrara: Vascular endothelial growth factor is a secreted angiogenic mitogen. *Science*, 246, 1306-9 (1989)

47. Ciardiello, F., R. Bianco, R. Caputo, R. Caputo, V. Damiano, T. Troiani, D. Melisi, F. De Vita, S. De Placido, A. R. Bianco & G. Tortora: Antitumor activity of ZD6474, a vascular endothelial growth factor receptor tyrosine kinase inhibitor, in human cancer cells with acquired resistance to antiepidermal growth factor receptor therapy. *Clin Cancer Res*, 10, 784-93 (2004)

48. Prewett, M., J. Huber, Y. Li, A. Santiago, W. O'Connor, K. King, J. Overholser, A. Hooper, B. Pytowski, L. Witte, P. Bohlen & D. J. Hicklin: Antivascular endothelial growth factor receptor (fetal liver kinase 1) monoclonal antibody inhibits tumor angiogenesis and growth of several mouse and human tumors. *Cancer Res*, 59, 5209-18 (1999)

49. Watanabe, H., A. J. Mamelak, E. Weiss, B. Wang, I. Freed, A. K. Brice, L. Wachtman, K. L. Gabrielson, N. Yokota, D. J. Hicklin, R. S. Kerbel, M. Haas & D. N. Sauder: Anti-vascular endothelial growth factor receptor-2 antibody accelerates renal disease in the NZB/W F1 murine systemic lupus erythematosus model. *Clin Cancer Res*, 11, 407-9 (2005)

50. Wedge, S. R., D. J. Ogilvie, M. Dukes, J. Kendrew, J. O. Curwen, L. F. Hennequin, A. P. Thomas, E. S. Stokes, B. Curry, G. H. Richmond & P. F. Wadsworth: ZD4190: an orally active inhibitor of vascular endothelial growth factor signaling with broad-spectrum antitumor efficacy. *Cancer Res*, 60, 970-5 (2000)

51. Wood, J. M., G. Bold, E. Buchdunger, R. Cozens, S. Ferrari, J. Frei, F. Hofmann, J. Mestan, H. Mett, T. O'Reilly, E. Persohn, J. Rosel, C. Schnell, D. Stover, A. Theuer, H. Towbin, F. Wenger, K. Woods-Cook, A. Menrad, G. Siemeister, M. Schirner, K. H. Thierauch, M. R. Schneider, J. Drevs, G. Martiny-Baron & F. Totzke: PTK787/ZK 222584, a novel and potent inhibitor of vascular endothelial growth factor receptor tyrosine kinases, impairs vascular endothelial growth factor-induced responses and tumor growth after oral administration. *Cancer Res*, 60, 2178-89 (2000)

52. Vaisman, N., D. Gospodarowicz & G. Neufeld: Characterization of the receptors for vascular endothelial growth factor. *J Biol Chem*, 265, 19461-6 (1990)

53. Miller, J. C., H. H. Pien, D. Sahani, A. G. Sorensen & J. H. Thrall: Imaging angiogenesis: applications and potential for drug development. *J Natl Cancer Inst*, 97, 172-87 (2005)

54. Blankenberg, F. G., M. V. Backer, Z. Levashova, V. Patel & J. M. Backer: *In vivo* tumor angiogenesis imaging with site-specific labeled (99m)Tc-HYNIC-VEGF. *Eur J Nucl Med Mol Imaging*, 33, 841-8 (2006)

55. Blankenberg, F. G., S. Mandl, Y. A. Cao, C. O'Connell-Rodwell, C. Contag, C. Mari, T. I. Gaynutdinov, J. L. Vanderheyden, M. V. Backer & J. M. Backer: Tumor imaging using a standardized radiolabeled adapter protein

docked to vascular endothelial growth factor. *J Nucl Med*, 45, 1373-80 (2004)

56. Cai, W., K. Chen, K. A. Mohamedali, Q. Cao, S. S. Gambhir, M. G. Rosenblum & X. Chen: PET of vascular endothelial growth factor receptor expression. *J Nucl Med*, 47, 2048-56 (2006)

57. Chan, C., J. Sandhu, A. Guha, D. A. Scollard, J. Wang, P. Chen, K. Bai, L. Lee & R. M. Reilly: A human transferrin-vascular endothelial growth factor (hnTf-VEGF) fusion protein containing an integrated binding site for (111)In for imaging tumor angiogenesis. *J Nucl Med*, 46, 1745-52 (2005)

58. Collingridge, D. R., V. A. Carroll, M. Glaser, E. O. Aboagye, S. Osman, O. C. Hutchinson, H. Barthel, S. K. Luthra, F. Brady, R. Bicknell, P. Price & A. L. Harris: The development of ((124)I)iodinated-VG76e: a novel tracer for imaging vascular endothelial growth factor *in vivo* using positron emission tomography. *Cancer Res*, 62, 5912-9 (2002)

59. Cornelissen, B., R. Oltenfreiter, V. Kersemans, L. Staelens, F. Frankenne, J. M. Foidart & G. Slegers: *In vitro* and *in vivo* evaluation of (123I)-VEGF165 as a potential tumor marker. *Nucl Med Biol*, 32, 431-6 (2005)

60. Li, S., M. Peck-Radosavljevic, O. Kienast, J. Preitfellner, E. Havlik, W. Schima, T. Traub-Weidinger, S. Graf, M. Beheshti, M. Schmid, P. Angelberger & R. Dudczak: Iodine-123-vascular endothelial growth factor-165 (123I-VEGF165). Biodistribution, safety and radiation dosimetry in patients with pancreatic carcinoma. *Q J Nucl Med Mol Imaging*, 48, 198-206 (2004)

61. Lu, E., W. R. Wagner, U. Schellenberger, J. A. Abraham, A. L. Klibanov, S. R. Woulfe, M. M. Csikari, D. Fischer, G. F. Schreiner, G. H. Brandenburger & F. S. Villanueva: Targeted *in vivo* labeling of receptors for vascular endothelial growth factor: approach to identification of ischemic tissue. *Circulation*, 108, 97-103 (2003)

62. Yoshimoto, M., S. Kinuya, A. Kawashima, R. Nishii, K. Yokoyama & K. Kawai: Radioiodinated VEGF to image tumor angiogenesis in a LS180 tumor xenograft model. *Nucl Med Biol*, 33, 963-9 (2006)

63. Backer, M. V., Z. Levashova, V. Patel, B. T. Jehning, K. Claffey, F. G. Blankenberg & J. M. Backer: Molecular imaging of VEGF receptors in angiogenic vasculature with single-chain VEGF-based probes. *Nat Med*, 13, 504-9 (2007)

64. Virostko, J., J. Xie, D. E. Hallahan, C. L. Arteaga, J. C. Gore & H. C. Manning: A molecular imaging paradigm to rapidly profile response to angiogenesis-directed therapy in small animals. *Mol Imaging Biol*, 11, 204-12 (2009)

65. Ferrara, N.: Vascular endothelial growth factor: basic science and clinical progress. *Endocr Rev*, 25, 581-611 (2004)

66. Kerr, J. F., A. H. Wyllie & A. R. Currie: Apoptosis: a basic biological phenomenon with wide-ranging implications in tissue kinetics. *Br J Cancer*, 26, 239-57 (1972)

67. Earnshaw, W. C., L. M. Martins & S. H. Kaufmann: Mammalian caspases: structure, activation, substrates, and functions during apoptosis. *Annu Rev Biochem*, 68, 383-424 (1999)

68. Weinberg, R. A.: The Biology of Cancer. Garland Science, Taylor & Francis Group, New York (2007)

69. Zhou, L. & D. C. Chang: Dynamics and structure of the Bax-Bak complex responsible for releasing mitochondrial proteins during apoptosis. *J Cell Sci*, 121, 2186-96 (2008)

70. Thornberry, N. A. & Y. Lazebnik: Caspases: enemies within. *Science*, 281, 1312-6 (1998)

71. Hengartner, M. O.: The biochemistry of apoptosis. *Nature*, 407, 770-6 (2000)

72. Blankenberg, F. G.: *In vivo* detection of apoptosis. *J Nucl Med*, 49 Suppl 2, 81S-95S (2008)

73. Gaipl, U. S., T. D. Beyer, I. Baumann, R. E. Voll, C. M. Stach, P. Heyder, J. R. Kalden, A. Manfredi & M. Herrmann: Exposure of anionic phospholipids serves as anti-inflammatory and immunosuppressive signal--implications for antiphospholipid syndrome and systemic lupus erythematosus. *Immunobiology*, 207, 73-81 (2003)

74. Bialik, S. & A. Kimchi: Autophagy and tumor suppression: recent advances in understanding the link between autophagic cell death pathways and tumor development. *Adv Exp Med Biol*, 615, 177-200 (2008)

75. de Bruin, E. C. & J. P. Medema: Apoptosis and non-apoptotic deaths in cancer development and treatment response. *Cancer Treat Rev*, 34, 737-49 (2008)

76. Kelekar, A.: Introduction to the review series Autophagy in Higher Eukaryotes--a matter of survival or death. *Autophagy*, 4, 555-6 (2008)

77. Castedo, M., J. L. Perfettini, T. Roumier, K. Andreau, R. Medema & G. Kroemer: Cell death by mitotic catastrophe: a molecular definition. *Oncogene*, 23, 2825-37 (2004)

78. Blankenberg, F. G.: Molecular imaging: The latest generation of contrast agents and tissue characterization techniques. *J Cell Biochem*, 90, 443-53 (2003)

79. Haas, R. L., D. de Jong, R. A. Valdes Olmos, C. A. Hoefnagel, I. van den Heuvel, S. F. Zerp, H. Bartelink & M. Verheij: *In vivo* imaging of radiation-induced apoptosis in follicular lymphoma patients. *Int J Radiat Oncol Biol Phys*, 59, 782-7 (2004)

80. Kartachova, M., R. L. Haas, R. A. Olmos, F. J. Hoebers, N. van Zandwijk & M. Verheij: *In vivo* imaging of apoptosis by 99mTc-Annexin V scintigraphy: visual

analysis in relation to treatment response. *Radiother Oncol*, 72, 333-9 (2004)

81. Loose, D., H. Vermeersch, F. De Vos, P. Deron, G. Slegers & C. Van de Wiele: Prognostic value of 99mTc-HYNIC annexin-V imaging in squamous cell carcinoma of the head and neck. *Eur J Nucl Med Mol Imaging*, 35, 47-52 (2008)

82. Rottey, S., D. Loose, L. Vakaet, C. Lahorte, H. Vermeersch, S. Van Belle & C. Van de Wiele: 99mTc-HYNIC Annexin-V imaging of tumors and its relationship to response to radiotherapy and/or chemotherapy. *Q J Nucl Med Mol Imaging*, 51, 182-8 (2007)

83. Vermeersch, H., H. Ham, S. Rottey, C. Lahorte, F. Corsetti, R. Dierckx, N. Steinmetz & C. Van de Wiele: Intraobserver, interobserver, and day-to-day reproducibility of quantitative 99mTc-HYNIC annexin-V imaging in head and neck carcinoma. *Cancer Biother Radiopharm*, 19, 205-10 (2004)

84. Kietselaer, B. L., C. P. Reutelingsperger, H. H. Boersma, G. A. Heidendal, I. H. Liem, H. J. Crijns, J. Narula & L. Hofstra: Noninvasive detection of programmed cell loss with 99mTc-labeled annexin A5 in heart failure. *J Nucl Med*, 48, 562-7 (2007)

85. Thimister, P. W., L. Hofstra, I. H. Liem, H. H. Boersma, G. Kemerink, C. P. Reutelingsperger & G. A. Heidendal: *In vivo* detection of cell death in the area at risk in acute myocardial infarction. *J Nucl Med*, 44, 391-6 (2003)

86. Rongen, G. A., W. J. Oyen, B. P. Ramakers, N. P. Riksen, O. C. Boerman, N. Steinmetz & P. Smits: Annexin A5 scintigraphy of forearm as a novel *in vivo* model of skeletal muscle preconditioning in humans. *Circulation*, 111, 173-8 (2005)

87. Kietselaer, B. L., C. P. Reutelingsperger, G. A. Heidendal, M. J. Daemen, W. H. Mess, L. Hofstra & J. Narula: Noninvasive detection of plaque instability with use of radiolabeled annexin A5 in patients with carotid-artery atherosclerosis. *N Engl J Med*, 350, 1472-3 (2004)

88. Blankenberg, F. G., J. Kalinyak, L. Liu, M. Koike, D. Cheng, M. L. Goris, A. Green, J. L. Vanderheyden, D. C. Tong & M. A. Yenari: 99mTc-HYNIC-annexin V SPECT imaging of acute stroke and its response to neuroprotective therapy with anti-Fas ligand antibody. *Eur J Nucl Med Mol Imaging*, 33, 566-74 (2006)

89. Lorberboym, M., F. G. Blankenberg, M. Sadeh & Y. Lampl: *In vivo* imaging of apoptosis in patients with acute stroke: correlation with blood-brain barrier permeability. *Brain Res*, 1103, 13-9 (2006)

90. Lampl, Y., M. Lorberboym, F. G. Blankenberg, M. Sadeh & R. Gilad: Annexin V SPECT imaging of phosphatidylserine expression in patients with dementia. *Neurology*, 66, 1253-4 (2006)

91. Ohnishi, S., J. L. Vanderheyden, E. Tanaka, B. Patel, A. M. De Grand, R. G. Laurence, K. Yamashita & J. V. Frangioni: Intraoperative detection of cell injury and cell death with an 800 nm near-infrared fluorescent annexin V derivative. *Am J Transplant*, 6, 2321-31 (2006)

92. Schellenberger, E. A., R. Weissleder & L. Josephson: Optimal modification of annexin V with fluorescent dyes. *Chembiochem*, 5, 271-4 (2004)

93. Balasubramanian, K., B. Mirnikjoo & A. J. Schroit: Regulated externalization of phosphatidylserine at the cell surface: implications for apoptosis. *J Biol Chem*, 282, 18357-64 (2007)

94. Balasubramanian, K. & A. J. Schroit: Aminophospholipid asymmetry: A matter of life and death. *Annu Rev Physiol*, 65, 701-34 (2003)

95. Elliott, J. I., A. Surprenant, F. M. Marelli-Berg, J. C. Cooper, R. L. Cassady-Cain, C. Wooding, K. Linton, D. R. Alexander & C. F. Higgins: Membrane phosphatidylserine distribution as a non-apoptotic signalling mechanism in lymphocytes. *Nat Cell Biol*, 7, 808-16 (2005)

96. Reshef, A., A. Shirvan, R. N. Waterhouse, H. Grimberg, G. Levin, A. Cohen, L. G. Ulysse, G. Friedman, G. Antoni & I. Ziv: Molecular imaging of neurovascular cell death in experimental cerebral stroke by PET. *J Nucl Med*, 49, 1520-8 (2008)

97. Zhou, D., W. Chu, J. Rothfuss, C. Zeng, J. Xu, L. Jones, M. J. Welch & R. H. Mach: Synthesis, radiolabeling, and *in vivo* evaluation of an 18F-labeled isatin analog for imaging caspase-3 activation in apoptosis. *Bioorg Med Chem Lett*, 16, 5041-6 (2006)

98. Summy, J. M. & G. E. Gallick: Treatment for advanced tumors: SRC reclaims center stage. *Clin Cancer Res*, 12, 1398-401 (2006)

99. Mintorovitch, J., M. E. Moseley, L. Chileuitt, H. Shimizu, Y. Cohen & P. R. Weinstein: Comparison of diffusion- and T2-weighted MRI for the early detection of cerebral ischemia and reperfusion in rats. *Magn Reson Med*, 18, 39-50 (1991)

100. Moseley, M. E., Y. Cohen, J. Mintorovitch, L. Chileuitt, H. Shimizu, J. Kucharczyk, M. F. Wendland & P. R. Weinstein: Early detection of regional cerebral ischemia in cats: comparison of diffusion- and T2-weighted MRI and spectroscopy. *Magn Reson Med*, 14, 330-46 (1990)

101. Dzik-Jurasz, A., C. Domenig, M. George, J. Wolber, A. Padhani, G. Brown & S. Doran: Diffusion MRI for prediction of response of rectal cancer to chemoradiation. *Lancet*, 360, 307-8 (2002)

102. Cui, Y., X. P. Zhang, Y. S. Sun, L. Tang & L. Shen: Apparent diffusion coefficient: potential imaging biomarker for prediction and early detection of response to

chemotherapy in hepatic metastases. *Radiology*, 248, 894-900 (2008)

103. Koh, D. M., E. Scurr, D. Collins, B. Kanber, A. Norman, M. O. Leach & J. E. Husband: Predicting response of colorectal hepatic metastasis: value of pretreatment apparent diffusion coefficients. *AJR Am J Roentgenol*, 188, 1001-8 (2007)

104. Seierstad, T., K. Roe & D. R. Olsen: Noninvasive monitoring of radiation-induced treatment response using proton magnetic resonance spectroscopy and diffusion-weighted magnetic resonance imaging in a colorectal tumor model. *Radiother Oncol*, 85, 187-94 (2007)

105. Kim, H., D. E. Morgan, H. Zeng, W. E. Grizzle, J. M. Warram, C. R. Stockard, D. Wang & K. R. Zinn: Breast tumor xenografts: diffusion-weighted MR imaging to assess early therapy with novel apoptosis-inducing anti-DR5 antibody. *Radiology*, 248, 844-51 (2008)

106. Moffat, B. A., T. L. Chenevert, T. S. Lawrence, C. R. Meyer, T. D. Johnson, Q. Dong, C. Tsien, S. Mukherji, D. J. Quint, S. S. Gebarski, P. L. Robertson, L. R. Junck, A. Rehemtulla & B. D. Ross: Functional diffusion map: a noninvasive MRI biomarker for early stratification of clinical brain tumor response. *Proc Natl Acad Sci U S A*, 102, 5524-9 (2005)

107. Hall, D. E., B. A. Moffat, J. Stojanovska, T. D. Johnson, Z. Li, D. A. Hamstra, A. Rehemtulla, T. L. Chenevert, J. Carter, D. Pietronigro & B. D. Ross: Therapeutic efficacy of DTI-015 using diffusion magnetic resonance imaging as an early surrogate marker. *Clin Cancer Res*, 10, 7852-9 (2004)

108. Lee, K. C., S. Sud, C. R. Meyer, B. A. Moffat, T. L. Chenevert, A. Rehemtulla, K. J. Pienta & B. D. Ross: An imaging biomarker of early treatment response in prostate cancer that has metastasized to the bone. *Cancer Res*, 67, 3524-8 (2007)

109. Yankeelov, T. E., M. Lepage, A. Chakravarthy, E. E. Broome, K. J. Niermann, M. C. Kelley, I. Meszoely, I. A. Mayer, C. R. Herman, K. McManus, R. R. Price & J. C. Gore: Integration of quantitative DCE-MRI and ADC mapping to monitor treatment response in human breast cancer: initial results. *Magn Reson Imaging*, 25, 1-13 (2007)

110. Morse, D. L., J. P. Galons, C. M. Payne, D. L. Jennings, S. Day, G. Xia & R. J. Gillies: MRI-measured water mobility increases in response to chemotherapy via multiple cell-death mechanisms. *NMR Biomed*, 20, 602-14 (2007)

111. Colvin, D. C., T. E. Yankeelov, M. D. Does, Z. Yue, C. Quarles & J. C. Gore: New insights into tumor microstructure using temporal diffusion spectroscopy. *Cancer Res*, 68, 5941-7 (2008)

112. Volkow, N. D., G. J. Wang, F. Telang, J. S. Fowler, J. Logan, A. R. Childress, M. Jayne, Y. Ma & C. Wong: Dopamine increases in striatum do not elicit craving in cocaine abusers unless they are coupled with cocaine cues. *Neuroimage*, 39, 1266-73 (2008)

113. Mukherjee, J., B. T. Christian, K. A. Dunigan, B. Shi, T. K. Narayanan, M. Satter & J. Mantil: Brain imaging of 18F-fallypride in normal volunteers: blood analysis, distribution, test-retest studies, and preliminary assessment of sensitivity to aging effects on dopamine D-2/D-3 receptors. *Synapse*, 46, 170-88 (2002)

114. Farde, L., S. Pauli, H. Hall, L. Eriksson, C. Halldin, T. Hogberg, L. Nilsson, I. Sjogren & S. Stone-Elander: Stereoselective binding of 11C-raclopride in living human brain--a search for extrastriatal central D2-dopamine receptors by PET. *Psychopharmacology (Berl)*, 94, 471-8 (1988)

115. Peterson, L. M., D. A. Mankoff, T. Lawton, K. Yagle, E. K. Schubert, S. Stekhova, A. Gown, J. M. Link, T. Tewson & K. A. Krohn: Quantitative imaging of estrogen receptor expression in breast cancer with PET and 18F-fluoroestradiol. *J Nucl Med*, 49, 367-74 (2008)

116. Linden, H. M., S. A. Stekhova, J. M. Link, J. R. Gralow, R. B. Livingston, G. K. Ellis, P. H. Petra, L. M. Peterson, E. K. Schubert, L. K. Dunnwald, K. A. Krohn & D. A. Mankoff: Quantitative fluoroestradiol positron emission tomography imaging predicts response to endocrine treatment in breast cancer. *J Clin Oncol*, 24, 2793-9 (2006)

117. Eiblmaier, M., L. A. Meyer, M. A. Watson, P. M. Fracasso, L. J. Pike & C. J. Anderson: Correlating EGFR expression with receptor-binding properties and internalization of 64Cu-DOTA-cetuximab in 5 cervical cancer cell lines. *J Nucl Med*, 49, 1472-9 (2008)

118. Klapper, L. N., M. H. Kirschbaum, M. Sela & Y. Yarden: Biochemical and clinical implications of the ErbB/HER signaling network of growth factor receptors. *Adv Cancer Res*, 77, 25-79 (2000)

119. Olayioye, M. A., R. M. Neve, H. A. Lane & N. E. Hynes: The ErbB signaling network: receptor heterodimerization in development and cancer. *Embo J*, 19, 3159-67 (2000)

120. Zhang, H., A. Berezov, Q. Wang, G. Zhang, J. Drebin, R. Murali & M. I. Greene: ErbB receptors: from oncogenes to targeted cancer therapies. *J Clin Invest*, 117, 2051-8 (2007)

121. Nicholson, R. I., J. M. Gee & M. E. Harper: EGFR and cancer prognosis. *Eur J Cancer*, 37 Suppl 4, S9-15 (2001)

122. Wong, A. J., S. H. Bigner, D. D. Bigner, K. W. Kinzler, S. R. Hamilton & B. Vogelstein: Increased expression of the epidermal growth factor receptor gene in malignant gliomas is invariably associated with gene amplification. *Proc Natl Acad Sci U S A*, 84, 6899-903 (1987)

123. Libermann, T. A., H. R. Nusbaum, N. Razon, R. Kris, I. Lax, H. Soreq, N. Whittle, M. D. Waterfield, A. Ullrich & J. Schlessinger: Amplification, enhanced expression and possible rearrangement of EGF receptor gene in primary human brain tumours of glial origin. *Nature*, 313, 144-7 (1985)

124. Mulloy, R., A. Ferrand, Y. Kim, R. Sordella, D. W. Bell, D. A. Haber, K. S. Anderson & J. Settleman: Epidermal growth factor receptor mutants from human lung cancers exhibit enhanced catalytic activity and increased sensitivity to gefitinib. *Cancer Res*, 67, 2325-30 (2007)

125. Salomon, D. S., R. Brandt, F. Ciardiello & N. Normanno: Epidermal growth factor-related peptides and their receptors in human malignancies. *Crit Rev Oncol Hematol*, 19, 183-232 (1995)

126. Ciardiello, F., R. Caputo, T. Troiani, G. Borriello, E. R. Kandimalla, S. Agrawal, J. Mendelsohn Mendelsohn, A. R. Bianco & G. Tortora: Antisense oligonucleotides targeting the epidermal growth factor receptor inhibit proliferation, induce apoptosis, and cooperate with cytotoxic drugs in human cancer cell lines. *Int J Cancer*, 93, 172-8 (2001)

127. Gill, G. N., T. Kawamoto, C. Cochet, A. Le, J. D. Sato, H. Masui, C. McLeod & J. Mendelsohn: Monoclonal anti-epidermal growth factor receptor antibodies which are inhibitors of epidermal growth factor binding and antagonists of epidermal growth factor binding and antagonists of epidermal growth factor-stimulated tyrosine protein kinase activity. *J Biol Chem*, 259, 7755-60 (1984)

128. Wu, X., Z. Fan, H. Masui, N. Rosen & J. Mendelsohn: Apoptosis induced by an anti-epidermal growth factor receptor monoclonal antibody in a human colorectal carcinoma cell line and its delay by insulin. *J Clin Invest*, 95, 1897-905 (1995)

129. Petit, A. M., J. Rak, M. C. Hung, P. Rockwell, N. Goldstein, B. Fendly & R. S. Kerbel: Neutralizing antibodies against epidermal growth factor and ErbB-2/neu receptor tyrosine kinases down-regulate vascular endothelial growth factor production by tumor cells *in vitro* and *in vivo*: angiogenic implications for signal transduction therapy of solid tumors. *Am J Pathol*, 151, 1523-30 (1997)

130. Perrotte, P., T. Matsumoto, K. Inoue, H. Kuniyasu, B. Y. Eve, D. J. Hicklin, R. Radinsky & C. P. Dinney: Anti-epidermal growth factor receptor antibody C225 inhibits angiogenesis in human transitional cell carcinoma growing orthotopically in nude mice. *Clin Cancer Res*, 5, 257-65 (1999)

131. Ciardiello, F., R. Caputo, R. Bianco, V. Damiano, G. Pomatico, S. De Placido, A. R. Bianco & G. Tortora: Antitumor effect and potentiation of cytotoxic drugs activity in human cancer cells by ZD-1839 (Iressa), an epidermal growth factor receptor-selective tyrosine kinase inhibitor. *Clin Cancer Res*, 6, 2053-63 (2000)

Abbreviations: FLT: fluorothymidine, PET: positron emission tomography, TK1: thymidine kinase 1, Rb: retinoblastoma gene product, ppRb: hypophosphorylated retinoblastoma gene product, CRC: colorectal cancer, WT: wild type, ATP: adenosine triphosphate, 5-FU: 5-fluorouracil, FDG: (18F)2-fluoro-2-deoxy-D-glucose, CT: computed tomography, SUV: standardized uptake value, ROI: region of interest, DCE-MRI: dynamic contrast enhanced magnetic resonance imaging, VEGF: vascular endothelial growth factor, mAb: monoclonal antibody, TKI: tyrosine kinase inhibitor, SPECT: single photon emission computed tomography, NIR: near-infrared, PARP: poly-ADP-ribose polymerase, PS: phosphotidyl serine, TNF: tumor necrosis factor, FasL: Fas ligand, ADC: apparent diffusion coefficient, MRI: magnetic resonance imaging, OGSE: oscillating gradient spin-echo, FES: fluoroestrodiol, EGFR: endothelial growth factor receptor, MAPK: mitogen activated protein kinase, PI3K: phosphoinositide 3-kinase, TGF alpha: transforming growth factor alpha, IL-8: interleukin-8, bFGF: basic fibroblast growth factor

Key Words: molecular imaging, cancer, FLT, thymidine kinase 1 (TK1), PET, FDG, DCE, MRI, ADC, annexin, apoptosis, angiogenesis, review

Send correspondence to: H. Charles Manning, Vanderbilt University Institute of Imaging Science (VUIIS), Vanderbilt University Medical School, 1161 21st Avenue South, AA 1105 MCN, Nashville, TN 37232, Tel: 615-322-3793, Fax: 615-322-0734, E-mail: henry.c.manning@vanderbilt.edu

http://www.bioscience.org/current/vol16.htm